NONCOHERENT CODED CONTINUOUS PHASE MODULATION

Lutz H.-J. Lampe, Robert Schober, Gerald Enzner, Johannes B. Huber

Laboratorium für Nachrichtentechnik, Universität Erlangen–Nürnberg
Cauerstraße 7, D–91058 Erlangen, Germany
e-mail: *LLampe@LNT.de*, WWW: *http://www.LNT.de/LNT2*

***Abstract* — Continuous phase modulation (CPM) systems for noncoherent coded transmission are proposed and analyzed. Specifically, the application of a feedback–free modulator is regarded. For demodulation, a receiver structure which requires only two or three linear filters is considered. For decoding, noncoherent sequence estimation (NSE) with Viterbi decoding and per–survivor processing is applied. Noteworthy, in our approach the problems of low–complexity filtering and reduced–state decoding can be treated separately. Since we give a recursive formula for the phase reference symbol necessary for NSE metric calculation, computational effort is further decreased. Overall, in terms of complexity, the proposed noncoherent receiver provides significant advantages over recently presented approaches. The high performance of the novel noncoherent CPM system is confirmed by simulation results.**

1. Introduction

Continuous phase modulation (CPM) [1] is an attractive technique for digital communications. Due to its constant envelope, full amplifier power can be exploited without any back–off to avoid amplifier nonlinearities. Additionally, the power efficiency of CPM is improved by the inherent trellis code caused by smoothed phase transitions [2, 3]. For the same reason, CPM is highly bandwidth efficient, too. In combination with CPM, noncoherent reception is appealing since the need for explicit phase synchronization is avoided. In particular, *noncoherent sequence estimation (NSE)* techniques are very well suited to channels with time–variant phases [4, 5].
In this paper, we show how power and bandwidth efficiency of noncoherent CPM is improved by proper combination with convolutional coding. To limit the complexity of the noncoherent receiver, we first regard a convenient CPM signal representation. Starting from the decomposition approach for CPM [6, 2, 3], the receiver front–end presented in [7] is applied. Thus, in contrast to previous approaches, e.g. [8], the problems of low–complex filtering and reduced–state NSE can be treated separately. Furthermore, from the decomposition of CPM it becomes obvious how to employ codes matched to *feedback–free* CPM, cf. e.g. [2, 9, 10, 11]. We show that for reduced–state NSE it suffices to expand the state definition of the underlying channel code by only a *single* information symbol to account for the memory of CPM and channel phase.
For noncoherent CPM, we apply a novel NSE scheme which has been previously proposed for coded M–ary phase–shift keying (MPSK) [12] and differential MPSK (MDPSK) transmission over intersymbol interference channels [13]. This NSE scheme enables the recursive calculation of the reference symbol required for metric calculation and thus, offers considerable savings in computational complexity for achieving the same/better power efficiency as/than in [8]/[14]. Simulation results verify that the proposed noncoherent coded CPM scheme enables power–efficient transmission with a very fair demodulation and decoding complexity.

2. Transmission System

2.1. CPM Signal Representation

The passband CPM signal has the form [1]

$$s_{\mathrm{HF}}(\boldsymbol{a},t)=\sqrt{\frac{2E_s}{T}}\cos\left(2\pi f_c t+2\pi h\sum_{i=0}^{\infty}a[i]q(t-iT)\right), \quad (1)$$

where f_c is the carrier frequency, E_s denotes the signal energy per modulation interval T, $h=k/p$ is the rational modulation index with relatively prime integers k and p. The information sequence $\boldsymbol{a}=\langle a[i]\rangle$, $i\in\mathbb{N}_0$, consists of M–ary elements $a[i]\in\{\pm1,\pm3,\ldots,\pm(M-1)\}$, M even. The *phase pulse* $q(t)$ is normalized as usual such that $q(t)=0$ for $t\leq 0$ and $q(t)=1/2$ for $t\geq LT$.
For a compact representation of $s_{\mathrm{HF}}(\boldsymbol{a},t)$ as an equivalent complex baseband (ECB) signal it is convenient to use the transformation frequency $f_0=f_c-h\cdot\frac{M-1}{2T}$, cf. [2, 3, 7], which is different from the carrier frequency f_c. Furthermore, we introduce the modified data sequence $\boldsymbol{\beta}$ with components

$$\beta[i]\stackrel{\triangle}{=}(a[i]+M-1)/2 \quad \in\{0,1,\ldots,M-1\}. \quad (2)$$

Then, the ECB signal $s(\boldsymbol{\beta},t)$ can be interpreted as a sequence of time–limited signal segments $\rho(\boldsymbol{b}[i],t)$:

$$s(\boldsymbol{\beta},t)=\sum_{i=0}^{\infty}\rho(\boldsymbol{b}[i],t-iT) \quad (3)$$

with $\rho(\boldsymbol{b}[i],t)=0$ for $t\notin[0,T)$ and address vector $\boldsymbol{b}[i]$, which is generated from $\boldsymbol{\beta}$ by a minimum trellis encoder [3, 7]. In particular, using the decomposition approach of CPM [2, 3], a description with pM^L signal elements $\rho(\boldsymbol{b}[i],t)$ addressed by vector

$$\boldsymbol{b}[i]\stackrel{\triangle}{=}[\beta[i],\ldots,\beta[i-L+1],\psi[i-L]] \quad (4)$$

from a trellis with pM^{L-1} states $S[i]\stackrel{\triangle}{=}[\beta[i-1],\ldots,\beta[i-L+1],\psi[i-L]]$ is always possible. The *phase state*

$$\psi[i-L]\stackrel{\triangle}{=}\left(k\sum_{m=0}^{i-L}\beta[m]\right)\bmod p\,,\ \psi[i]\in\{0,\ldots,p-1\} \quad (5)$$

subsumizes the contributions of all past modulator input data for which the phase pulses have already reached a constant value. The data symbols $(\beta[i], \ldots, \beta[i-L+1])$ determine the phase transient, cf. [7]. Correspondingly, this CPM Modulator is subsequently referred to as CPM with *frequency mapping*. Due to (5) the inherent trellis encoder contains a recursive structure, which is analogous to the well–known differential encoder necessary for generation of DPSK from PSK. Generally, for CPM this differential encoder is essential to resolve phase ambiguities.

2.2. Phase–State Mapping and Coding

In the above description of CPM, data symbols are mapped to phase changes. However, a mapping to the absolute phase is also possible, cf. [2]. For the interesting special case $M = p$ the unique relation

$$(k \cdot \beta[i]) \bmod p = (\psi[i] - \psi[i-1]) \bmod p \qquad (6)$$

(cf. (5)) allows to express the information by the signal phase at the end of the corresponding modulation interval. With the address vector

$$\boldsymbol{w}[i] \triangleq [\psi[i], \ldots, \psi[i-L]] \qquad (7)$$

a modified signal table can be used. That is, the operation (6) is incorporated into the signal table definition and now, the signal elements are denoted by $\rho(\boldsymbol{w}[i], t)$. Since the information is represented in the absolute phase, this structure is referred to as CPM with *phase–state mapping* [2]. Phase–state mapping is generated immediately by application of a discrete–time differentiator to the CPM modulator input symbols (Eq. (6))[1].

Of course, by applying such a differentiation the phase ambiguities due to the rotational invariance of CPM become unresolvable. Therefore, it should never be applied when using a coherent receiver with an explicit carrier phase synchronization unit, because a phase slip would cause a complete loss until a training sequence (e.g. frame synchronization word) appears. The situation is quite different for a noncoherent receiver combined with a convolutional encoder. Here, phase ambiguities are resolvable due to a noncoherently non–catastrophic encoder [4, 15]. As phase estimation is part of the noncoherent decoding process, actual phase slips do not exist. They simply correspond to detours in the trellis decoding algorithm. Our investigations showed that most of the known codes optimized for coherent transmission are rotationally variant, i.e., noncoherently non–catastrophic.

Phase–state mapping is perfectly matched to coded CPM using convolutional codes. For the sake of simplicity, we restrict ourselves to nonrecursive convolutional encoders with obvious minimum encoder structure. Due to the feedback–free shift register structure of the CPM encoder, a fusion of the convolutional and the CPM encoder is possible, cf. e.g. [2, 9, 10, 11]. Compared to frequency mapping, more delay elements can be shared by both encoders. Thus, with phase–state mapping a greater coding gain can be achieved for the same decoder complexity [2]. Moreover, although the distance properties and the probability of Viterbi decoding error events are the same for both mapping strategies, with the non–recursive structure the number of erroneous decisions per error event is decreased [3].

[1]More generally, for $M = p^{\mu}$, $\mu \in \mathbb{N}$, a semi–differential mapping is proposed in [3], where differentiation is applied to the least significant p–ary digit of the data symbols.

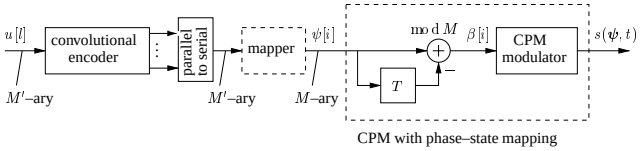

Figure 1: Transmitter structure for coded CPM with phase–state mapping. $M = p$.

Subsequently, we concentrate on CPM with phase–state mapping. Therefore, we consider the sequence $\boldsymbol{\psi}$ of phase states as input to the modified CPM modulator (i.e., the combination of differentiator and original CPM modulator) with signal elements $\rho(\boldsymbol{w}[i], t)$. Accordingly, the CPM signal is denoted by $s(\boldsymbol{\psi}, t)$. Furthermore, let $u[l]$ denote M'–ary information symbols entering the convolutional encoder. Clearly, the clocks of the time–indices l and i are related through the code rate R_c and the sizes M', M of the respective symbol alphabets. In case of binary codes ($M' = 2$) and $M > 2$, some combining of encoder and modulator, e.g., via mapping, is required to obtain phase states $\psi[i]$, cf. e.g. [2, 9]. The application of M–ary convolutional codes also for $M > 2$ is a more natural way to encode M–ary CPM, cf. e.g. [11, 16]. Here, the information symbols $u[l]$ are taken from an M–ary alphabet and the convolutional encoder delivers immediately phase states $\psi[i]$. The transmitter structure of coded CPM with phase–state mapping is depicted in Fig. 1.

2.3. Channel

We consider transmission over the additive white Gaussian noise (AWGN) channel with a signal phase unknown to the receiver. The received signal $r(t)$ may then be written as

$$r(t) = \mathrm{e}^{\mathrm{j}\phi(t)} \cdot s(\boldsymbol{\psi}, t) + n(t) \;, \qquad (8)$$

where the unknown phase $\phi(t)$ is slowly time–varying and $n(t)$ denotes complex–valued AWGN with two–sided power spectral density N_0 in the ECB domain (corresponding to a physical channel noise with one–sided power spectral density N_0, as usual).

2.4. Receiver Structure

For the optimum receiver, a bank of $D \leq 2 \cdot M^L$ matched filters is required to deliver sufficient statistics for $r(t)$ [1]. In addition, detection has to be done by maximum–likelihood sequence estimation (MLSE) based on a super–trellis, which takes into account error correction coding, the trellis structure inherent to CPM, and the dependences among received samples due to the unknown channel phase (see Section 3). If both filtering and sequence estimation are optimally solved, a very high computational complexity results. Thus, suboptimum receiver structures and signal processing requiring a low complexity are desired, whereas performance degradation should remain as small as possible. In contrast to previous approaches, e.g. [8], we treat these two problems separately. Doing so, for a given complexity the highest performance is achieved. The employed NSE scheme will be described in detail in Section 3.

Clearly, for a low receiver complexity a set of D basis functions which represent the signal space spanned by $\rho(\boldsymbol{w}[i],t)$ as completely as possible for a given (small) value of D has to be found. For this purpose, we adopt the reduction methods proposed by Huber and Liu [7] leading to a compact receiver front–end with very simple filter realizations. In [7] it is shown that the signal elements of almost all CPM schemes relevant in practice can be sufficiently represented by only $D = 2$ or $D = 3$ complex exponential functions of duration T. More specifically, the signal elements $\rho(\boldsymbol{w}[i],t)$ in the ECB domain are approximated by

$$\rho(\boldsymbol{w}[i],t) \approx \sum_{d=1}^{D} \rho_d(\boldsymbol{w}[i])\mathrm{e}^{\mathrm{j}2\pi f_d t} \tag{9}$$

with $f_d = \frac{\Delta f}{2}(2d-1-D) + h\frac{M-1}{2T}$, $\quad 1 \le d \le D$. Here, $\rho_d(\boldsymbol{w}[i])$ are the coordinates of $\rho(\boldsymbol{w}[i],t)$ with respect to the chosen basis of the CPM signal space, and Δf denotes the frequency spacing parameter. The rational behind (9) is that time–limited functions can be well represented by samples in the frequency domain and using $\sin(\pi fT)/(\pi fT)$ functions for interpolation. Apparently, the frequency spacing parameter Δf has to be optimized for maximum utilizable free Euclidean distance, for details we refer to [7]. The vector $\boldsymbol{\rho}(\boldsymbol{w}[i]) \triangleq [\rho_1(\boldsymbol{w}[i]),\ldots,\rho_D(\boldsymbol{w}[i])]$ of coordinates is obtained from

$$\boldsymbol{\rho}(\boldsymbol{w}[i]) = [\varrho_1(\boldsymbol{w}[i]),\ldots,\varrho_D(\boldsymbol{w}[i])]\cdot\boldsymbol{C}^{-1}\ , \tag{10}$$

where $\varrho_d(\boldsymbol{w}[i])$ are the *spectral samples* at frequency f_d

$$\varrho_d(\boldsymbol{w}[i]) = \int_0^T \rho(\boldsymbol{w}[i],t)\mathrm{e}^{\mathrm{j}2\pi f_d t}\,\mathrm{d}t\ , \quad 1 \le d \le D\ , \tag{11}$$

and $\boldsymbol{C}$ is the covariance matrix of the D exponential basis functions.

The D samples of the received signal at the i^{th} modulation interval are arranged in the vector $\boldsymbol{r}[i] \triangleq [r_1[i],\ldots,r_D[i]]$ with

$$r_d[i] = \int_0^T r(t+iT)\mathrm{e}^{\mathrm{j}2\pi f_d t}\,\mathrm{d}t\ , \quad 1 \le d \le D\ . \tag{12}$$

Noteworthy, the used receiver front end allows direct application of noncoherent detection methods used for linear modulation schemes, e.g. [4, 5, 13], i.e., a whitening filter necessary for the scheme in [8] is not required (see Section 3). In addition, a main benefit of using time–limited complex exponential functions as basis is that very low–complex timing synchronization can be accomplished easily [17, 18].

3. Noncoherent Sequence Estimation for CPM

Now, optimum noncoherent sequence estimation (NSE) and suboptimum NSE with windowing of the observations are briefly described. Specifically, we introduce the concepts of a finite rectangular and an infinite, but exponentially decaying observation window. For derivation of the NSE metric for CPM we assume the unknown channel phase to be constant, i.e., $\phi(t) = \phi$. Later on, this restriction is relieved, and in the simulations presented in Section 4, the influence of a time–varying phase on the receiver performance is also investigated.

For a constant envelope signal and the AWGN channel with unknown phase the optimum NSE metric for a block of N_T transmitted symbols $\psi[i]$, $0 \le i \le N_T-1$, reads [19, 5]

$$\Lambda[N_T-1] = \Re\left\{\sum_{i=1}^{N_T-1} \boldsymbol{r}[i]\cdot\boldsymbol{\rho}^H(\tilde{\boldsymbol{w}}[i])\cdot\tilde{q}_{\mathrm{ref}}^*[i-1]\right\}\ , \tag{13}$$

with the definition $\tilde{q}_{\mathrm{ref}}[i-1] \triangleq \sum_{m=0}^{i-1} \boldsymbol{r}[m]\cdot\boldsymbol{\rho}^H(\tilde{\boldsymbol{w}}[m])$ and $\tilde{\boldsymbol{w}}[i]$ constructed from $\tilde{\psi}[i]$ (7), which correspond via encoding to hypothetical trial data symbols $\tilde{u}[l]$. $\tilde{q}_{\mathrm{ref}}[i-1]$ can be considered as *phase reference symbol*. From (13) the *incremental* metric $\lambda[i] \triangleq \Lambda[i+1]-\Lambda[i]$ at time i, $0 \le i \le N_T-2$, follows as

$$\lambda[i] = \Re\left\{\boldsymbol{r}[i]\cdot\boldsymbol{\rho}^H(\tilde{\boldsymbol{w}}[i])\cdot\tilde{q}_{\mathrm{ref}}^*[i-1]\right\} \tag{14}$$

In its present form, $\tilde{q}_{\mathrm{ref}}[i-1]$ corresponds to an unlimited phase memory, which grows with time i. Hence, a tree search has to be employed for maximization of $\Lambda[N_T-1]$, cf. [20]. Moreover, the channel phase is required to be constant during the whole transmission time, which is usually not true in practice, of course.

To overcome these drawbacks, limitation of the phase memory has been proposed. Specifically, rectangular windowing [5] with window size $N \ge 2$, i.e., $\tilde{q}_{\mathrm{ref}}[i-1]$ is approximated by

$$\tilde{q}_{\mathrm{ref}}[i-1] \triangleq \frac{1}{N-1}\cdot\sum_{m=1}^{N-1} \boldsymbol{r}[i-m]\cdot\boldsymbol{\rho}^H(\tilde{\boldsymbol{w}}[i-m])\ , \tag{15}$$

and exponential windowing [12, 13] with forgetting factor α, $0 \le \alpha < 1$, where the modified reference symbol is generated *recursively* from

$$\tilde{q}_{\mathrm{ref}}[i-1] \triangleq \alpha\cdot\tilde{q}_{\mathrm{ref}}[i-2]+(1-\alpha)\boldsymbol{r}[i-1]\boldsymbol{\rho}^H(\tilde{\boldsymbol{w}}[i-1])\ , \tag{16}$$

are promising approaches. Apparently, for the special cases $N = 2$ ($N \to \infty$) and $\alpha = 0$ ($\alpha \to 1$) (15) and (16) are identical.

In terms of computational complexity, exponential windowing compares favorably with rectangular windowing [13]. For the former technique less arithmetic operations are necessary, and moreover, complexity is independent of α. For rectangular windowing, however, complexity increases with N.

Clearly, now NSE can be performed by a full–state Viterbi algorithm in a super trellis taking into account the memory of convolutional coding, of CPM, and of the phase reference. In order to limit complexity of noncoherent CPM decoding, we employ per–survivor processing [21] and define a trellis diagram with $(M')^K$ states $S'[l] \triangleq (\tilde{u}[l-1],\ldots,\tilde{u}[l-K])$, $K \ge 0$. Here, the value of K determines the exchange between performance and complexity. For $0 \le m \le K$, the hypothetical symbols $\tilde{u}[l-m]$ are defined by the transition from state $S'[l]$ to $S'[l+1]$. For $m > K$, the symbols $\tilde{u}[l-m]$ are taken from the surviving path terminating in state $S'[l]$. In case of exponential windowing, each path in the trellis has its private reference symbol $\tilde{q}_{\mathrm{ref}}[i-1]$, which is updated according to (16) using the previous reference symbol $\tilde{q}_{\mathrm{ref}}[i-2]$ of the same path. At the end of each trellis branch only the reference symbol associated with the surviving path is stored and used for calculation of the first reference symbol of the next branch.

4. Simulation Results

To demonstrate the performance of the proposed noncoherent coded CPM transmission scheme, simulations of the bit–error rate (BER) versus E_b/N_0 (E_b: received signal energy per information bit) have been performed. For the first simulations, the channel phase $\phi(t)$ is kept constant.

First of all, a performance comparison with other CPM schemes is mandatory. In particular, noncoherent CPM systems recently published by Colavolpe and Raheli [8] and Raphaeli and Divsalar [14] show promising results. Unfortunately, in [8] only uncoded CPM is discussed, and thus the results cannot be used for comparison. But adopting the proposed receiver structure to CPM with frequency mapping we have achieved very similar performance for the same number of NSE trellis states as in [8]. Moreover, we would like to mention that the metric computation according to (13) provides an additional complexity advantage over [8]. In contrast to [8, Eq. (27)], not the absolute value, but only the real part of a complex number has to be calculated.

In [14], 4–ary CPFSK with $h = 1/4$ and coding with a 4–state binary rate 1/2 code (generator polynomials $\boldsymbol{g}_1 = (5)$, $\boldsymbol{g}_2 = (7)$ (base–8 representation)) is simulated. Two different reduced–state decoding algorithms, the so–called BDFA and EFDFA, are used. Noteworthy, the metric used in [14] is not the same as the one applied here (cf. Section 3), since a somewhat different approach for NSE is chosen in [14]. Whereas the BDFA is identical to the Viterbi algorithm with per–survivor processing, and thus decoder complexity is the same as for the reduced–state NSE scheme with rectangular windowing introduced in Section 3, the EFDFA requires a 4–5 times larger complexity, cf. [14].

We have adopted the system parameters of [14] for CPM with phase–state mapping, using only $D = 2$ complex filters (9) (the number of used filters is not specified in [14]), and the proposed NSE scheme with rectangular windowing (15). In Figs. 2a), b) the obtained BER curves are plotted over E_b/N_0. The results presented in [14, Fig. 11] are also shown (indicated by R&D); for BDFA with 8 and 32 states and $N = 10$ in Fig. 2a) and for EFDFA with 8 states and various N in Fig. 2b). For the reference curve of coherent CPM, Viterbi decoding in an 8–state trellis is performed, which completely describes the combined memory of the code and CPM. For the proposed noncoherent CPM, decoding with 8 states (Fig. 2a)) and 16 states (Fig. 2b)) using per–survivor processing is considered (cf. Section 3).

Regarding Fig. 2a), it is apparent that for similar complexity the CPM receiver of [14] with BDFA is clearly outperformed by the proposed technique. The number of states for BDFA has to be increased to 32 in order to achieve the same power efficiency as our proposal with 8 states. Now the curves in Fig. 2b) are considered. Although EFDFA uses only half the number of states, the overall decoding complexity is still more than twice the complexity of the proposed decoding algorithm based on per–survivor processing. Remarkably, this reduced complexity does not lead to a performance loss. For $N = 3$, even a gain of about 0.4 dB at BER $\approx 10^{-3}$ is obtained. The slight disadvantage for $N = 20$ probably results from a larger number $D > 2$ of receive filters used in [14], because the respective curve intersects with the curve of coherent CPM with $D = 2$.

As an important example of coded binary CPM with $h = 1/2$,

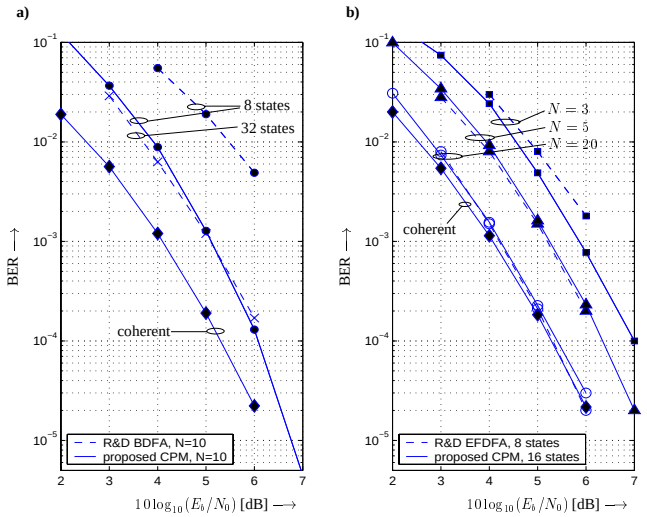

Figure 2: BER of the proposed CPM receiver scheme compared to the scheme in [14] (R&D). 4–ary CPFSK with $h = 1/4$ and a 4–state binary rate 1/2 code. a): R&D with BDFA, $N = 10$. b): R&D with EFDFA, various N.

we consider Gaussian minimum shift keying (GMSK) with 3 dB–bandwidth–bit duration product $BT = 0.3$. For coding, the binary rate 1/2 convolution code with 16 states (generator polynomials $\boldsymbol{g}_1 = (2, 3)$, $\boldsymbol{g}_2 = (3, 5)$ (base–8 representation)) from [4, Table I] is taken. At the receiver, a front end with $D = 2$ filters is applied. NSE and coherent MLSE are performed on a trellis with 32 states, i.e., again for NSE per–survivor processing is employed. In case of coherent CPM, further expansion of states is not rewarding. The numerical results for noncoherent reception with rectangular and exponential windowing are presented in Figs. 3a) and b), respectively. Although states are reduced to a great extent, by increasing the observation interval of NSE, the performance of coherent reception with perfect phase synchronization is approached. This is true for both windowing techniques. Hence, the complexity advantages of exponential windowing can be fully exploited.

It is of high interest to discuss coded noncoherent multilevel CPM because, in the coherent case, best trade–off between power and bandwidth efficiency is found for 4 and 8–ary CPM. For this reason, we consider 2RC 4–ary CPM with $h = 1/4$, i.e., the frequency pulse $g(t) = \mathrm{d}q(t)/\mathrm{d}t$ is a raised cosine pulse with $L = 2$. A 4–ary rate 1/2 code with 16 states is chosen (generator polynomials $\boldsymbol{g}_1 = (1, 3, 3)$ and $\boldsymbol{g}_2 = (2, 3, 1)$ (base–4 representation)), which is also taken from [4, Table I]. Again, $D = 2$ is applied. For coherent reception of CPM, the joint code and modulator trellis has 64 states. NSE with per–survivor processing is performed on the same trellis, i.e., the state representation of the underlying code is expanded by only a single information symbol. As for GMSK, with $\phi(t) = \mathrm{const.}$, the proposed noncoherent CPM approaches the power–efficiency of coherent reception (without Figure). To assess the robustness of the proposed scheme to phase jitter, Fig. 4 shows the measured BER's as a function of σ_Δ for $E_b/N_0 = 5$ dB. Here, the phase $\phi(t)$ has been modeled as a Wiener process, i.e., the sequence of phase changes is a white Gaussian process with variance σ_Δ^2 over T cf. e.g. [18, 5, 14]. Clearly, there is a exchange be-

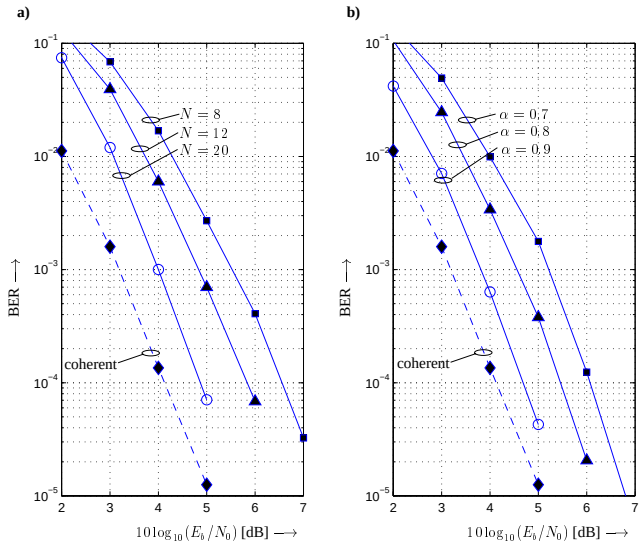

Figure 3: BER vs. E_b/N_0 for the proposed CPM system. GMSK with $BT = 0.3$ and a 16–state binary rate 1/2 code. NSE and coherent MLSE with 32 states, respectively. a) rectangular windowing. b) exponential windowing.

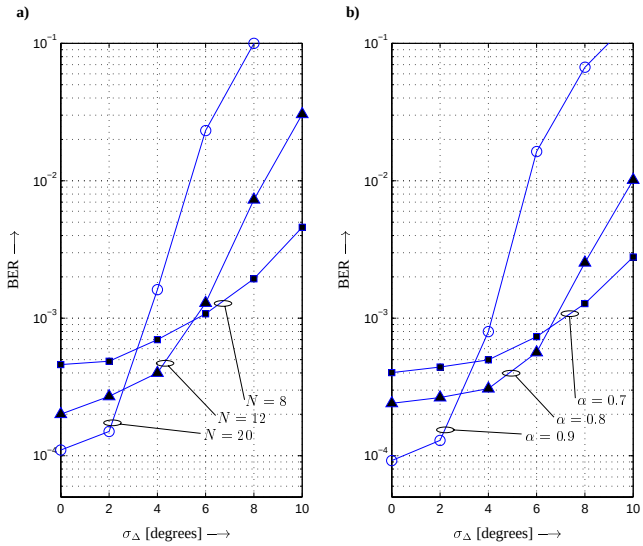

Figure 4: BER vs. the jitter standard deviation σ_Δ per modulation interval for the proposed CPM system. 2RC 4–ary CPM with $h = 1/4$ and a 16–state 4–ary rate 1/2 code. a) rectangular windowing. b) exponential windowing.

tween achievable power efficiency for $\sigma_\Delta = 0$ and robustness against phase noise. As α (N) increases, the robustness against phase variations deteriorates, while power efficiency for $\sigma_\Delta = 0$ improves. Consequently, in practice α (N) has to be adapted to the current situation. Since α is a real number, using the lower–complexity metric, for given E_b/N_0 and σ_Δ^2 the minimum achievable BER can always be attained exactly.

5. Conclusions

Coded noncoherent CPM transmission is discussed. At the transmitter, rotationally variant convolutional coding is efficiently combined with CPM. At the receiver, low–complexity filtering and Viterbi decoding with simple metrics for noncoherent reception are applied. For comparable complexity the proposed CPM system is shown to be superior to a recently presented scheme. Moreover, power efficiency of coherent CPM assuming perfect knowledge of the slowly time–varying channel phase is approached *without* increase of the number of trellis states. In summary, the proposed CPM scheme is attractive for power and bandwidth–efficient noncoherent transmission with very moderate complexity.

References

[1] J.B. Anderson, T. Aulin, and C.-E. Sundberg. *Digital Phase Modulation*. Plenum Press, New York, 1986.

[2] J.B. Huber and W. Liu. Convolutional Codes for CPM Using the Memory of the Modulation Process. In *Proc. IEEE Global Telecom. Conf.*, pages 43.1.1–43.1.5, Tokyo, 1987.

[3] B.E. Rimoldi. A Decomposition Approach to CPM. *IEEE Trans. Inf. Theory*, 34(2):260–270, March 1988.

[4] D. Raphaeli. Noncoherent Coded Modulation. *IEEE Trans. Com.*, 44:172–183, Feb. 1996.

[5] G. Colavolpe and R. Raheli. Noncoherent Sequence Detection. *IEEE Trans. Com.*, 47(9):1376–1385, September 1999.

[6] J.L. Massey. The How and Why of Channel Coding. In *Int. Zürich Sem. on Dig. Com.*, pp. E1.1–E1.7, Zürich, March 1984.

[7] J.B. Huber and W. Liu. An Alternative Approach to Reduced–Complexity CPM–Receivers. *IEEE J. Select. Areas Com.*, 7(9):1437–1449, December 1989.

[8] G. Colavolpe and R. Raheli. Noncoherent Sequence Detection of Continuous Phase Modulations. *IEEE Trans. Com.*, 47(9):1303–1307, September 1999.

[9] B.E. Rimoldi. Design of Coded CPFSK Modulation Systems for Bandwidth and Energy Efficiency. *IEEE Trans. Com.*, 37(9):897–905, September 1989.

[10] F. Morales-Moreno, W. Holubowicz, and S. Pasupathy. Optimization of Trellis Coded TFM Via Matched Codes. *IEEE Trans. Com.*, 42(2/3/4):867–876, February/March/April 1994.

[11] R.H.-H. Yang and D.P. Taylor. Trellis–Coded Continuous–Phase Frequency–Shift Keying with Ring Convolutional Codes. *IEEE Trans. Com.*, 40(4):1057–1067, July 1994.

[12] A. D'Andrea, U. Mengali, and G. Vitetta. Approximate ML Decoding of Coded PSK with No Explicit Carrier Phase Reference. *IEEE Trans. Com.*, 42:1033–1039, February/March/April 1994.

[13] R. Schober and W.H. Gerstacker. Metric for Noncoherent Sequence Estimation. *Electr. Letters*, 35(25):2178–2179, December 1999.

[14] D. Raphaeli and D. Divsalar. Multiple–Symbol Noncoherent Decoding of Uncoded and Convolutionally Coded Continuous Phase Modulation. *J. Commun. and Networks*, 4(1):238–248, December 1999.

[15] Y. Kofman, E. Zehavi, and S. Shamai (Shitz). *nd*–Convolutional Codes—Part II: Structural Analysis. *IEEE Trans. Inf. Theory*, 43(2):576–589, March 1997.

[16] B.E. Rimoldi and Q. Li. Coded Continuous Phase Modulation Using Ring Convolutional Codes. *IEEE Trans. Com.*, 43(11):2714–2720, November 1995.

[17] J.B. Huber and W. Liu. Data–Aided Synchronization of Coherent CPM–Receivers. *IEEE Trans. Com.*, 40(1):178–189, January 1992.

[18] M. Morelli, U. Mengali, and G.M. Vitetta. Joint Phase and Timing Recovery With CPM Signals. *IEEE Trans. Com.*, 45(7):867–876, July 1997.

[19] John G. Proakis. *Digital Communications*. McGraw–Hill, New York, third edition, 1995.

[20] S.T. Andersson and N.A.B. Svensson. Noncoherent Detection of Convolutionally Encoded Continuous Phase Modulation. *IEEE J. Select. Areas Com.*, 7(9):1402–1414, Dec. 1989.

[21] R. Raheli, A. Polydoros, and C.-K. Tzou. Per–Survivor Processing: A General Approach to MLSE in Uncertain Environments. *IEEE Trans. Com.*, 43:354–364, February/April 1995.